Science of the Total Environment 801 (2021) 149481

Contents lists available at ScienceDirect

Science of the Total Environment

journal homepage: www.elsevier.com/locate/scitotenv

Short Communication

Disentangling the role of ectomycorrhizal fungi in plant nutrient acquisition along a Zn gradient using X-ray imaging

Kaile Zhang [a,b], Ryan Tappero [c], Joske Ruytinx [d], Sara Branco [e], Hui-Ling Liao [a,b,*]

[a] North Florida Research and Education Center, University of Florida, Quincy, FL 32351, USA
[b] Soil and Water Science Department, University of Florida, Gainesville, FL 32611, USA
[c] Brookhaven National Laboratory, NSLS-II, Upton, NY 11973, USA
[d] Research Groups Microbiology and Plant Genetics, Vrije Universiteit Brussel, Pleinlaan 2, 1050 Brussel, Belgium
[e] Department of Integrative Biology, University of Colorado Denver, Denver, CO 80204, USA

HIGHLIGHTS

- *S. luteus* dually regulated Zn uptake of pine roots depending on external Zn level.
- Non-mycorrhizal pine roots exposed to high Zn indiscriminately take up Zn.
- The absorption pattern of Ca, Cu, and Zn in pine roots was similar across Zn levels.
- Fe uptake was negatively affected by Zn level within ectomycorrhizal pine root.
- Higher accumulation of nutrients was found in fungal sheath compared to Hartig net.

GRAPHICAL ABSTRACT

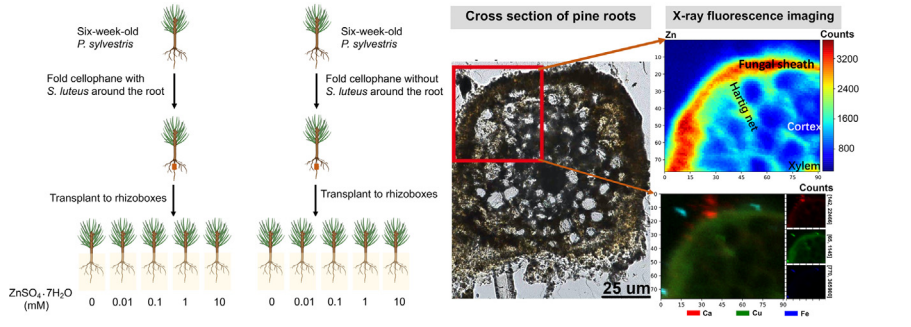

ARTICLE INFO

Article history:
Received 28 June 2021
Received in revised form 1 August 2021
Accepted 1 August 2021
Available online 8 August 2021

Editor: Jay Gan

Keywords:
Synchrotron X-ray fluorescence
Ectomycorrhizal fungi
Zn acquisition
Zn-other nutrient interactions
Suillus luteus
Pinus sylvestris

ABSTRACT

Zinc (Zn) is a plant essential micronutrient involved in a wide range of cellular processes. Ectomycorrhizal fungi (EMF) are known to play a critical role in regulating plant Zn status. However, how EMF control uptake and translocation of Zn and other nutrients in plant roots under different Zn conditions is not well known. Using X-ray fluorescence imaging, we found the EMF species *Suillus luteus* increased pine root Zn acquisition under low Zn concentrations and reduced its accumulation under higher Zn levels. By contrast, non-mycorrhizal pine roots exposed to high Zn indiscriminately take up and translocate Zn to root tissues, leading to Zn stress. Regardless of *S. luteus* inoculation, the absorption pattern of Ca and Cu was similar to Zn. Compared to Ca and Cu, effects of *S. luteus* on Fe acquisition were more marked, leading to a negative association between Zn addition and Fe concentration within EMF roots. Besides, higher nutrient accumulation in the fungal sheath, compared to hyphae inhabiting between intercellular space of cortex cells, implies the fungal sheath serves as a barrier to regulate nutrient transportation into fungal Hartig net. Our results demonstrate the crucial roles EMF play in plant nutrient uptake and how fungal partners ameliorate soil chemical conditions either by increasing or decreasing element uptake.

1. Introduction

Zinc (Zn) is one of the most abundant transition metals in organisms and an essential component of a wide range of proteins, membrane lipids, and DNA/RNA molecules in plants (Broadley et al., 2007). Zn plays key

* Corresponding author at: North Florida Research and Education Center, University of Florida, Quincy, FL 32351, USA.
E-mail address: sunny.liao@ufl.edu (H.-L. Liao).

https://doi.org/10.1016/j.scitotenv.2021.149481
0048-9697/

roles in plant growth, development, and defense (Cabot et al., 2019). It is the only metal involved in the six major enzyme classes (i.e., oxidoreductases, transferases, hydrolases, lyases, isomerases, ligases) (Palmer and Guerinot, 2009; Webb, 1992), serving as the structural or catalytic ion in a massive number of enzymes. Zn also contributes to ligand binding, protein folding, electron transfer, and nucleotide metabolism (Auld, 2001; Broadley et al., 2007; Maret, 2005; Takeda et al., 2018).

In plants, Zn uptake and the maintenance of Zn homeostasis are mainly governed by redox or chelation-based strategies (Palmer and Guerinot, 2009). The former is associated with the efflux of reductants, organic acids, and H^+ ions from Zn solubilizing microbes in the rhizosphere and plant cells. This enhances Zn-complex solubility and the release of Zn^{2+} for adsorption by microbes and root epidermal cells (Gupta et al., 2016; Mumtaz et al., 2017). Chelation, on the other hand, relies on Zn binding. It employs excretion of chelators or siderophores by roots and microorganisms to form Zn stable complexes that are subsequently transported into root epidermal cells (Ahmed and Holmström, 2014; Butaitė et al., 2017; Leventhal et al., 2019).

Ectomycorrhizal fungi (EMF) are obligate plant symbionts and crucial for host plant micro and macro-nutrient uptake (Read and Perez-Moreno, 2003; Smith and Read, 2010). These fungi dominate boreal and temperate forest ecosystems, including pine forests (Read and Perez-Moreno, 2003; Talbot et al., 2014). Several studies showed EMF can both regulate Zn uptake and Zn distribution in plant tissues under deficient and toxic conditions (Bücking and Heyser, 1994; Schutzendubel and Polle, 2002). For example, under Zn deficient conditions, EMF upregulate the SlZRT1 gene, which encodes a plasma membrane-located ZIP (Zrt/Irt-Like protein) transporter that facilitates fungal cellular uptake of Zn^{2+} (Coninx et al., 2017). In high Zn concentrations, EMF can buffer Zn transfer into their plant hosts (Adriaensen et al., 2006). Some studies showed that *Suillus* spp., such as *S. luteus*, play an important role in regulating plant Zn uptake and maintaining Zn homeostasis (Coninx et al., 2017; Muller et al., 2007; Ruytinx et al., 2017). Despite these findings, the way EMF manipulate the spatial distribution of Zn in plant root tissues under different soil Zn concentrations remains largely unknown.

Previous research pointed to the potential for EMF to regulating the uptake of mineral elements other than Zn (e.g., Mn, Cu, Cd, and Ni) and playing a critical role in plant survival both in benign and toxic environmental conditions (Adriaensen et al., 2005; Canton et al., 2016; Jourand et al., 2010; Krznaric et al., 2009). In addition, available nutrients can interact to shape fungal and plant uptake. For example, there is a close positive association between Zn:Cu ratio in fungal mycelia and soil, probably resulting from the similarities in uptake mechanisms for Zn and Cu which leads to balanced uptake of these nutrients by EMF (Vinichuk, 2013). Furthermore, Hart et al. (1998) reported that increment in Ca^{2+} concentration inhibited plant Zn^{2+} uptake, as Zn^{2+} and Ca^{2+} are divalent cations and compete for some plant metal transporters (such as IRT1) and non-selective cation channels (Gupta et al., 2016). However, it is still unclear if and how EMF shape host plant overall nutrient acquisition across the plant-mycorrhiza-rhizosphere interface with the increase in external Zn concentrations.

This study aims at providing empirical evidence about how EMF regulate nutrient uptake from external environments in EMF systems. We investigated environmental nutrient uptake in one EMF partnership under high and low Zn levels, as well as Zn spatial distribution along EMF and non-EMF roots. We studied the well-established EMF *Suillus* – *Pinus* model system (Bücking and Heyser, 1994; Liao et al., 2016) and used synchrotron-based imaging techniques to visualize the spatial distribution of nutrients in root tissues.

2. Methods and materials

2.1. Fungal culture preparation

The ectomycorrhizal fungus *Suillus luteus* (UH-Slu-OF3 isolate) was used as the inoculum in this study. *S. luteus* was isolated in 2000 from pine stands in Overpelt Belgium and kept at 4 °C in the culture collection of Hasselt University with half-yearly subculturing. Previous studies indicated that *S. luteus* had high EC50 values ranging from 0.9 to 17.8 mM (Colpaert et al., 2004; Muller et al., 2004). Detailed description of the isolate and sampling site can be found in Colpaert et al. (2004). The solid Modified-Melin-Norkrans (MMN) medium was used to maintain *the S. luteus* isolate (Marx, 1970). The culture was stored at 25 °C in the dark and was sub-cultured every month. To prepare the fungal inoculum, the fungal culture was grown on the MMN medium covered with a layer of sterile cellophane at 25 °C in the dark for 7 days.

2.2. Pine seedling preparation

The seeds of *Pinus sylvestris* were purchased from Sheffield's Seed Co., Inc. (Locke, NY). The source of seeds was from France. The protocols applied for seed surface sterilization, germination, and the growth of pine seedlings were according to Liao et al. (2016). After 1.5 months of germination, the seedlings were used for the rhizobox bioassay.

2.3. Rhizobox bioassay

We set up a *S. luteus* – *P. sylvestris* bioassay to investigate nutrient uptake and spatial distribution in EMF roots (Fig. S1). These species are obligate symbionts in nature and known to occur together both in Zn contaminated and non-contaminated soils (Op De Beeck et al., 2015). The *S. luteus* – *P. sylvestris* bioassay was set up using six-week-old pine seedlings inoculated with *S. luteus* mycelia. The growing conditions of pine plants prior to plant bioassay are described in the study of Liao et al. (2016). The healthy pine seedlings with similar growth performance (e.g., similar height and weight) were chosen for bioassay. Briefly, we grew mycelium on MMN medium topped with a layer of sterile cellophane membrane to allow for tissue collection. We cut the cellophane (200 mg) using a pair of sterile scissors and used it to wrap ~5 cm length of pine seedling roots. For controls, we folded the same area of sterile cellophane without fungal inoculum around roots. Seedlings were then transplanted into a rhizobox that was filled with 120 g of sterile play sand (see Table S1 for the chemical properties of play sand). Before filling, each set of play sand was treated with a $ZnSO_4.7H_2O$ gradient (0, 0.01, 0.1, 1, and 10 mM). In total, there were 10 combinations for pine seedlings w/wo *S. luteus* inoculation, with three replicates for each combination. In the no Zn addition treatment, the transplanted pine seedlings w/wo *S. luteus* fungal inoculum can be regarded as the positive and negative control, respectively. The bioassay was conducted in a growth chamber at 25 °C and 70% humidity and exposed to fluorescent LED lights (200 μmole m^{-2} s^{-1}) for 12 h per day. 1 ml sterile distilled deionized (DDI) water was applied for each rhizobox every two days. After 2 weeks of post-treatment, the seedlings treated with 10 mM $ZnSO_4.7H_2O$ showed symptoms of Zn toxicity and died (100% death rate). Dead pine samples were discarded. Four weeks after inoculation, the pine roots were visualized under a dissection microscope (Olympus CX43, Olympus Corporation, Japan). Over 40% of *S. luteus*-inoculated root tips were successfully colonized (data not shown but analyses were done on the colonized roots in the *Suillus* treatments).

2.4. Sample preparation for synchrotron X-ray microfluorescence imaging

We used synchrotron X-ray microfluorescence (μ-XRF) imaging to quantify the abundance and radial distribution in pine roots collected from each treatment. Lateral roots were washed twice in DI water at room temperature to remove adhering sand. Roots were placed into a well of OCT (optimal cutting temperature) embedding media (Tissue-Tek, www.sakuraus.com/), then rapidly cooled to −20°C for preparation of tissue cryo-sections. Root tissue (near 0.3 mm from the root tip) was cryotomed at −20°C to a thickness of 20 μm using a CM 1900 cryotome (Leica Microsystems, www.leica-microsystems.com/). Tissue

sections were mounted onto ultralene film (SPEX, www.spexcsp.com/) and placed into a sample desiccator to equilibrate in the dry nitrogen atmosphere prior to analysis by X–ray microprobe.

μ-XRF analysis was performed at the 5-ID (SRX) and 4-BM (XFM) Beamlines of the National Synchrotron Light Source (NSLS-II), Brookhaven National Laboratory, Upton, NY. X-ray fluorescence was measured using a Hitachi SDD detector with a 90° position to the incident beam. Mapping was performed in fly scanning mode with a fixed energy of 10.0 keV, a pixel size of 1.0 to 10 μm, and a dwell time of 500 ms/pixel. Before performing X-ray imaging, selected sections were freeze-dried under −20 °C for approximately an hour. We observed a total of 24 root tips, 3 per Zn/EMF treatment using low-resolution imaging, and one representative root tip per treatment was finally applied for high-resolution imaging. Total spectrum of each element (Zn, Ca, Cu, and Fe) across different treatments is shown in Fig. S2.

2.5. Data analysis

Mapping images and imaging data analysis were performed using the PyXRF software (Li et al., 2017). The fluorescence intensity counts of each element were translated to elemental abundance using National Institute of Standards and Technology standard 1833 (Pella et al., 1986), and knowledge of sample thickness and density (estimated 0.9 g/cm^3) were used to convert to elemental concentration (μg/g). The average concentration of nutrients in pine root tissues (epidermis/sheath, apoplast/Hartig net, and xylem) was the mean of detected spots using *mean* and *sd* functions. Linear models (Pearson correlation, *cor.test* function) were conducted to determine: (1) correlations between Zn additions and the concentration of Zn, Ca, Cu, and Fe in non-inoculated pine root, (2) correlations of Zn additions with Fe concentration in *S. luteus* inoculated pine roots, and (3) correlations of Zn concentration with other nutrients (Ca, Cu, and Fe) concentration across pine root tissues. Non-linear regressions were used to analyze the relationships between Zn additions and the concentration of Zn, Ca, and Cu in *S. luteus*-inoculated pine roots by simulating the measured elemental concentration (package: *basicTrendline*, *trendline* function). All statistical analyses were performed in R (version 3.5).

3. Results

3.1. Spatial distribution of Zn in non-EMF vs. EMF root tissues of P. sylvestris

Overall, we found increases in environmental Zn were accompanied by increased root Zn uptake and pronounced differences in Zn compartment levels. In the presence of *S. luteus*, significantly higher Zn root accumulation was observed at the low Zn treatments (Figs. 1, 3, and S3; Table 1).

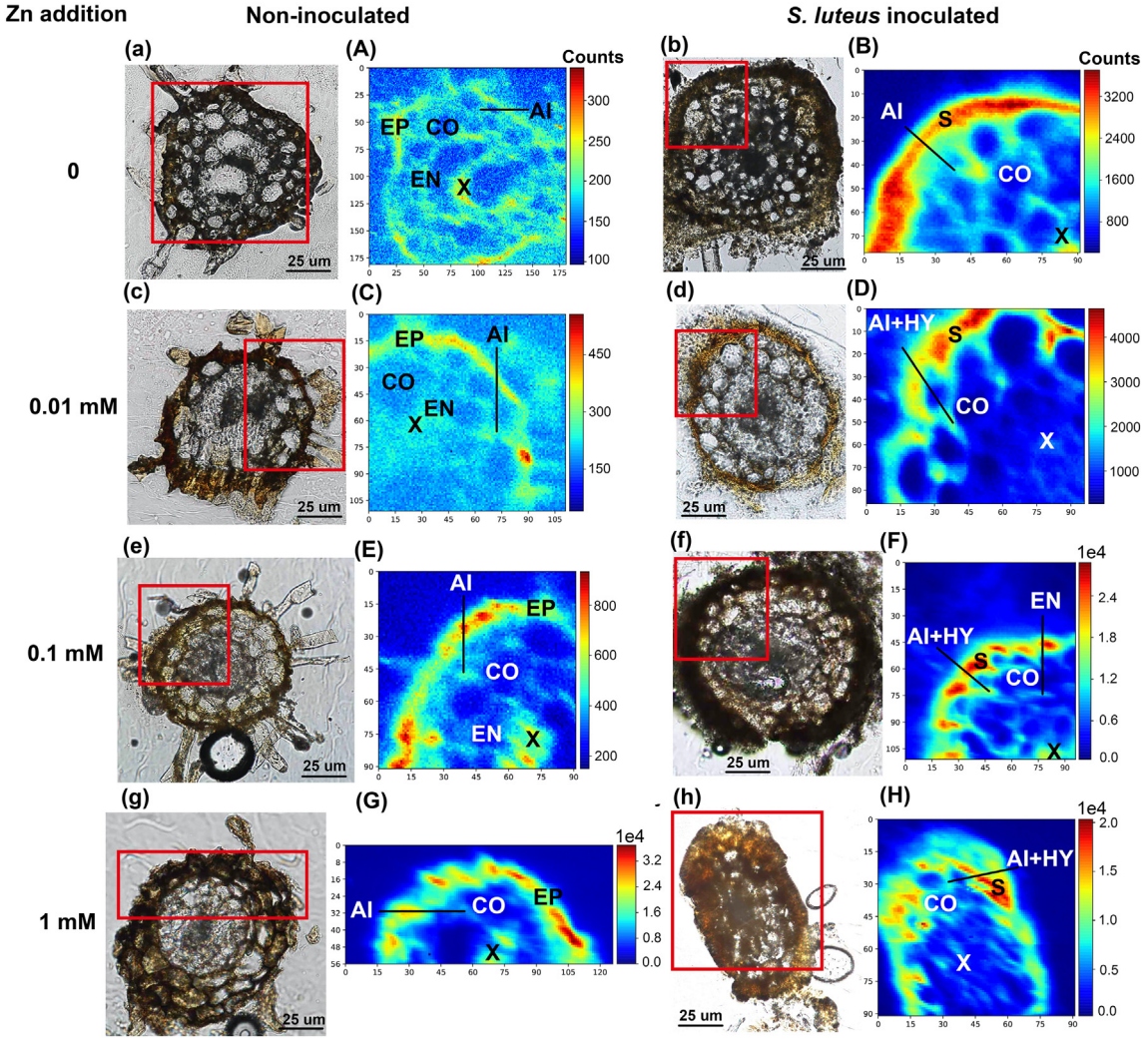

Fig. 1. High-resolution μ-XRF images of root cross sections (lowercase letters) and μ-XRF profiles (uppercase letters) across treatments. The latter highlights Zn levels (as shown by fluorescence counts per second) in root compartments across the different treatments. Each red rectangle marks the area of each root cross section corresponding to the area of X-ray imaging at its right panel. Abbreviations in μ-XRF images mark the pine root compartments. EP: epidermis; CO: cortex; EN: endodermis; X: xylem; Al: apoplastic space + intercellular space; HY: Hartig net; S: fungal sheath. (For interpretation of the references to color in this figure legend, the reader is referred to the web version of this article.)

Table 1
Average concentration (μg/g) of nutrients (Zn, Ca, Cu, and Fe) across compartments of pine root under different external Zn additions.

Zn addition		Total sample area[a]		Epidermis/sheath[b]		Apoplast/Hartig net[c]		Xylem	
		Concentration (μg/g)[d]							
		Blank[e]	*S. luteus*[f]	Blank	*S. luteus*	Blank	*S. luteus*	Blank	*S. luteus*
0	**Zn**	**16 ± 1**	**150 ± 6**	**19 ± 1**	**170 ± 2**	**13 ± 1**	**130 ± 2**	**18 ± 1**	**110 ± 2**
	Ca	318 ± 5	1,930 ± 75	559 ± 2	4,520 ± 33	246 ± 2	1,480 ± 10	397 ± 5	941 ± 9
	Cu	8	24 ± 1	13	28	1	19	7	17
	Fe	462 ± 20	2,060 ± 128	1,380 ± 13	3,850 ± 29	523 ± 7	1,560 ± 10	172 ± 3	331 ± 3
0.01 mM	**Zn**	**13 ± 1**	**110 ± 5**	**22 ± 1**	**210 ± 8**	**10**	**130 ± 3**	**13 ± 1**	**67 ± 2**
	Ca	1,530 ± 16	2,030 ± 158	3,150 ± 10	3,430 ± 20	869 ± 6	1,110 ± 17	1,120 ± 13	392 ± 3
	Cu	12	15	18	14	9	11	9	10
	Fe	252 ± 15	748 ± 10	743 ± 5	971 ± 9	272 ± 3	755 ± 10	29 ± 1	210 ± 2
0.1 mM	**Zn**	**36 ± 2**	**880 ± 10**	**39 ± 2**	**1,200 ± 8**	**19 ± 1**	**530 ± 6**	**33 ± 1**	**780 ± 4**
	Ca	420 ± 9	17,400 ± 485	740 ± 5	27,900 ± 326	214 ± 3	2,000 ± 28	360 ± 7	1,670 ± 22
	Cu	10	28 ± 1	11	32 ± 1	10	18	10	21
	Fe	377 ± 26	325 ± 17	1,350 ± 8	672 ± 13	277 ± 3	161 ± 2	296 ± 3	106 ± 2
1.0 mM	**Zn**	**860 ± 21**	**520 ± 9**	**1,500 ± 18**	**840 ± 5**	**500 ± 5**	**350 ± 3**	**800 ± 7**	**320 ± 4**
	Ca	1,760 ± 19	1,280 ± 74	2,460 ± 18	1,940 ± 20	1,040 ± 8	1,000 ± 8	1,500 ± 12	1,010 ± 10
	Cu	18 ± 1	19	22 ± 1	15	13	17	12	12
	Fe	2,560 ± 129	314 ± 18	4,590 ± 46	584 ± 6	221 ± 3	313 ± 5	83 ± 3	311 ± 4

Average concentration of nutrients in pine root tissues were the mean of detected spots.
[a] Total sample area includes fungal and pine tissue areas.
[b] Epidermis in the non-EMF root or sheath in the EMF root.
[c] Apoplast in the non-EMF root and Apoplast+Hartig net in the EM root.
[d] The data were rounded to the accepted significant digits according to NIST1833.
[e] Blank: non-inoculated treatments.
[f] *S. luteus*: *S. luteus*-inoculated treatments.

μ-XRF elemental mapping of non-EMF root cross sections under no Zn addition revealed that root Zn was obtained from the sand substrates (2.6 mg Zn/kg sands; Table S1), with Zn intensity of 16 μg/g in pine root tissues (Table 1). Zn mostly accumulated in epidermal cells (19 μg/g), apoplast (13 μg/g), and xylem (18 μg/g) (Table 1). As the Zn addition escalated, there was an increase in the total Zn accumulation in each compartment (Table 1, Fig. 3A, E, and I), with the average Zn concentration in these compartments soaring by over 40-fold from 0 to 1 mM Zn addition. Epidermal cells accumulated the greatest amount of Zn compared to other compartments (Table 1).

When pine seedlings were inoculated with *S. luteus*, we observed higher Zn accumulation in the fungal sheath (170 μg/g), apoplast and Hartig net (130 μg/g), and xylem (110 μg/g) in the no Zn addition treatment (Table 1). Increasing Zn concentration from 0 to 0.1 mM led to significantly increased Zn accumulation in these compartments (Fig. 3A, $R^2 = 0.88$; 3E, $R^2 = 0.95$; 3I, $R^2 = 0.97$; $P < 0.001$, Table 1). However, increase to 1 mM Zn substantially decreased Zn accumulation in these compartments. Across all Zn treatments (0 to 1 mM), the highest Zn concentration was observed in the fungal sheath. Compared to non-inoculated treatments, *S. luteus* significantly promoted Zn accumulation in pine root tissues under 0, 0.01, and 0.1 mM Zn conditions, with an increase of around 10 times. However, when treated with 1 mM Zn addition, inoculated samples yielded substantially lower Zn accumulation in these compartments than non-inoculated treatments.

3.2. Effects of Zn addition in the distribution of nutrients (Ca, Cu, and Fe) in colonized and non-colonized P. sylvestris roots

The fine spatial resolution of the μ-XRF images allowed us to identify and quantify other elements (e.g., Ca, Cu, and Fe) in root tissues along with Zn (Figs. 2 and S4). Regardless of *S. luteus* inoculation, the absorption pattern of Ca and Cu in pine root tissues was similar to Zn under the Zn addition gradient. Compared to Ca and Cu, the effect of *S. luteus* on Fe acquisition was more marked, leading to a negative association between Zn addition and Fe concentration within EMF roots (Figs. 2, 3, and S4; Table 1).

Also as seen in Zn, Ca, Cu, and Fe originating from sand substrates were primarily accumulated in epidermal cells/sheath, apoplast/Hartig net, and xylem irrespective of fungal colonization. Of these three elements, Cu had a lower concentration in root tissues. In non-EMF roots, Cu accumulation in the root tissues increased with the elevated external Zn concentration (Table 1; Fig. 3C, $R^2 = 0.35$; 3G, $R^2 = 0.05$; 3K, $R^2 = 0.43$; $P < 0.001$). When in the presence of *S. luteus*, the Cu accumulation in the fungal sheath and xylem increased with Zn addition elevating from 0 to 0.1 mM, while there was a contrasting trend following 1 mM Zn addition. In the apoplast and Hartig net, there was a small fluctuation for Zn accumulation against the Zn addition gradient of 0–1 mM.

Similar to Cu, we found positive relationships between Zn addition and Ca accumulation in root epidermis, apoplast, and xylem in non-EMF roots (Fig. 3B, $R^2 = 0.10$; 3F, $R^2 = 0.40$; 3J, $R^2 = 0.48$; $P < 0.001$). However, high Zn addition had a suppressing effect on the absorption of Ca in EMF roots. EMF root tissues accumulated greater Ca against the Zn addition gradient of 0–0.1 mM relative to non-EMF root tissues, whereas an opposite trend occurred under 1 mM Zn addition.

Zn addition was significantly associated with Fe accumulation in the epidermis/fungal sheath and xylem of root tissues. While tissue Fe increased in non-EMF roots, it decreased in the presence of *S. luteus* (Fig. 3D and L). Zn addition was negatively associated with Fe accumulation in the apoplast ($R^2 = 0.11$, $P < 0.001$)/Hartig net ($R^2 = 0.20$, $P < 0.001$) regardless of mycorrhizal status (Fig. 3H). Compared to Cu and Ca, the role of *S. luteus* in Fe absorption was more affected by external Zn concentration (Fig. 3).

4. Discussion

In this study, we showed *S. luteus* facilitated Zn accumulation in root tissues when pine seedlings are grown in relatively low external Zn concentrations (2.6–3.4 mg Zn/kg sand). This is consistent with previous discoveries of EMF contributing to micronutrient acquisition under deficient conditions (Canton et al., 2016; Vinichuk, 2013). When external Zn addition ranged from 0 to 0.1 mM, more Zn accumulated in the fungal sheath compared to the hyphae inhabiting between intercellular space of cortex cells, implying that the fungal sheath serves as a barrier to regulate the transportation of Zn into the fungal Hartig net. The same strategy may also be used by EMF to control Ca, Mg, and K uptake by EMF roots (Bücking et al., 2002).

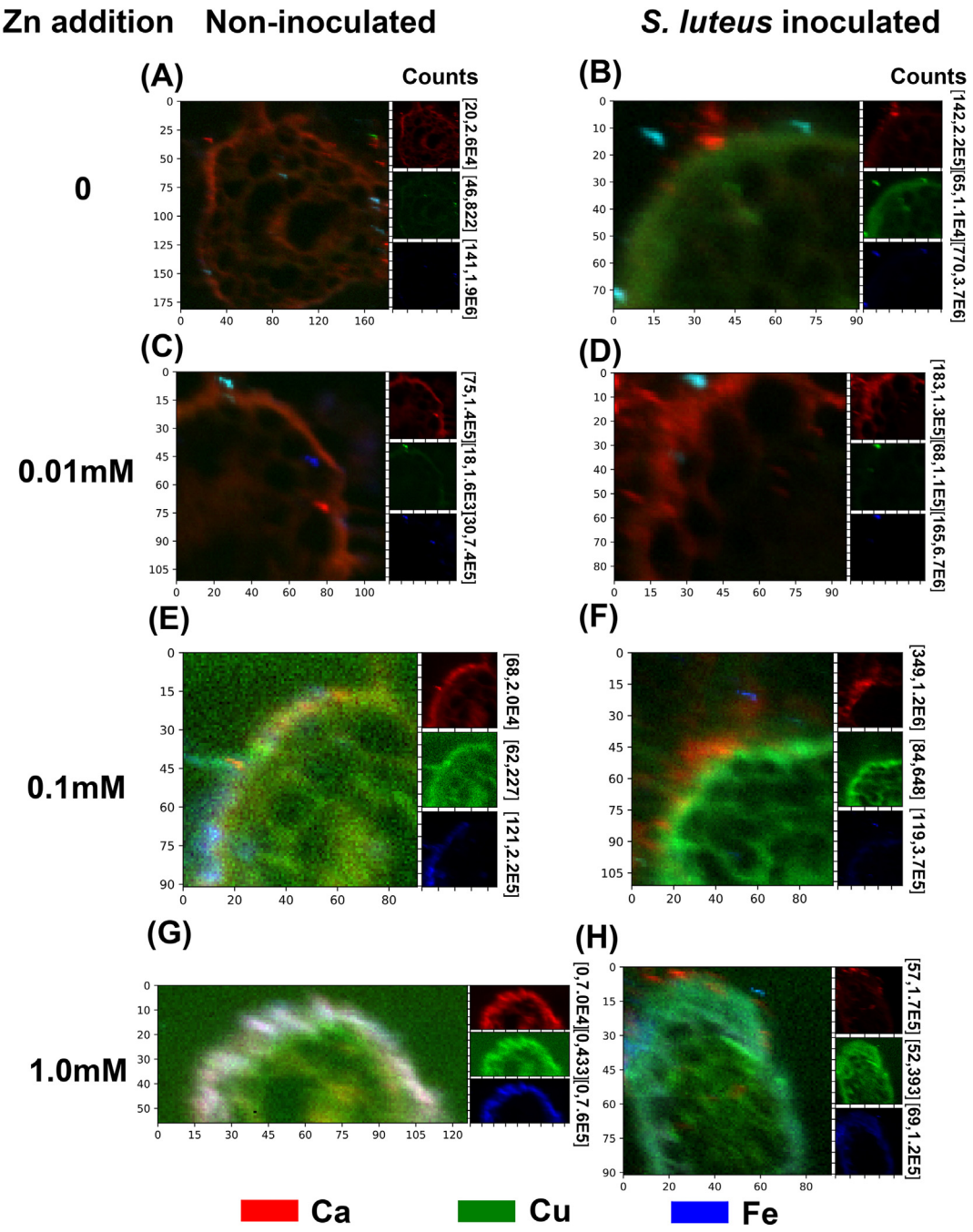

Fig. 2. μ-XRF mapping of Ca, Cu, and Fe intensity (shown by fluorescence counts per second) in root compartments across different treatments.

This study also showed that *S. luteus* was able to suppress Zn uptake under high external Zn concentration (10.6 mg Zn/kg sand), suggesting the fungus may control Zn uptake in both fungal and root tissues likely through detoxification mechanisms (Bui and Franken, 2018; Lin and Aarts, 2012). These mechanisms may enable EMF to shelter the plant roots from absorbing toxic levels of Zn. In fact, EMF can retain Zn in their mycelium, immobilize Zn, and subsequently buffer Zn from entering into their host plants under different Zn levels (Jentschke and Godbold, 2000). Denny and Wilkins (1987) exhibited that the extrametrical hyphae of *Paxillus involutus* accumulated far more Zn when *Betula* was exposed to high Zn concentrations (1.5 to 4.5 mM Zn) relative to the fungal sheath, cortex, and stele (including xylem) that had similar Zn accumulation. This is in part congruent with our result of reduced Zn accumulation in cortex cells and xylem with increased Zn addition. However, our study showed that fungal sheath had higher Zn accumulation than extrametrical hyphae, cortex, and xylem in response to external higher Zn concentration, which is partially different from the result of Denny and Wilkins (1987). It is likely that different EMF systems may rely on distinct strategies to protect the hosts against metal toxicity or alleviate metal toxicity in host plants. The pine seedlings in our study, nevertheless, were not able to survive under 82.6 mg Zn/kg sand concentration (10 mM Zn addition), indicating the *S. luteus* isolate, albeit Zn-tolerant isolate, used in our experiments has a limited ability to protect the pine host from Zn toxicity. By contrast, in non-EMF treatments, there was a positive association between Zn addition (0–1 mM) and Zn accumulation in pine root compartments (epidermis, cortical cells, and xylem). This indicates pines show no limitations in acquiring and translocating Zn to plant tissues at least until faced with Zn stress caused by elevated metal addition (referred to as a threshold level; Bücking and Heyser, 1994). Beyond the

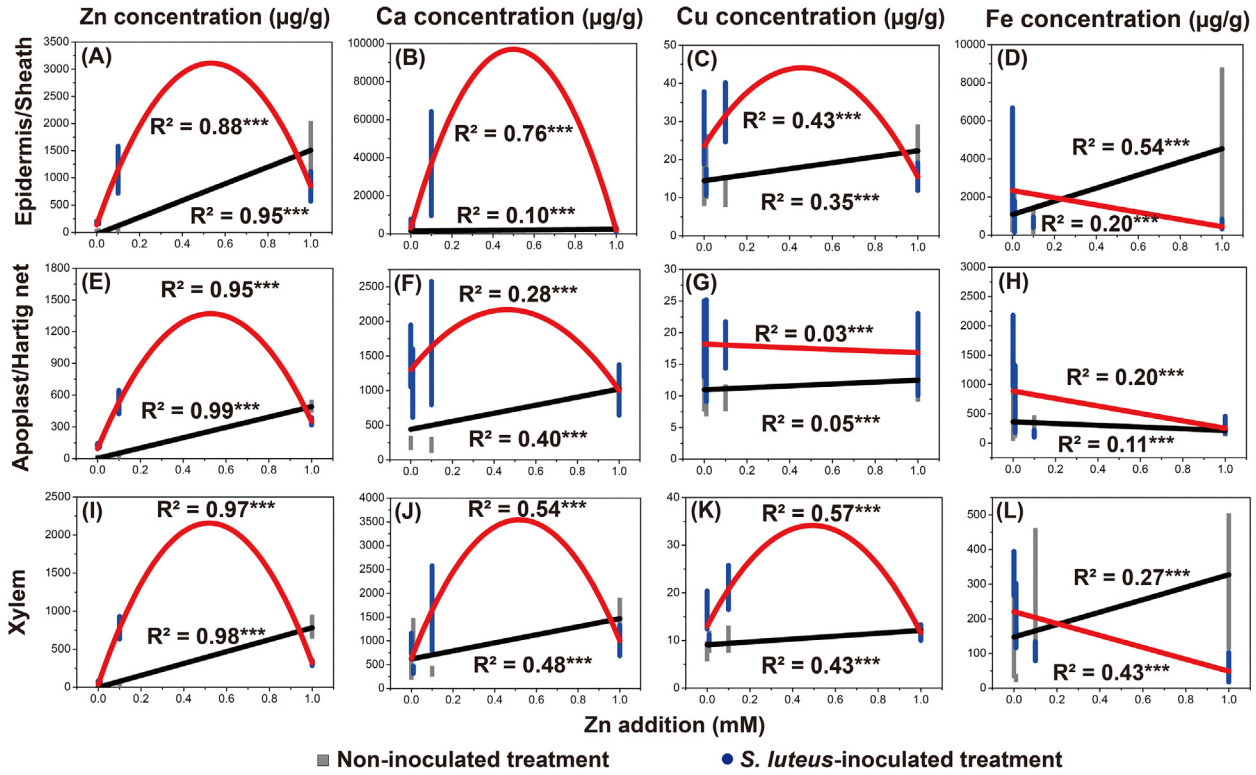

Fig. 3. The relationships between treated Zn concentration and the concentration of nutrients (Zn, Ca, Cu, and Fe) across compartments in pine root tissues under non- and *S. luteus* inoculated treatments. *** marks significance at $P < 0.001$. The data points indicate the nutrient concentration of root compartments with (in blue) and without (in grey) *S. luteus* inoculation. The curves in red and black indicate the change of nutrient concentration along the Zn gradient of 0–1 mM.

threshold level (10.6–82.6 mg Zn/kg sand in this study), the seedlings showed symptoms of Zn toxicity and were not able to survive after a few weeks post-treatment.

Along with Zn, Ca, Cu, and Fe have vital roles in the plant life cycle (Palmer and Guerinot, 2009). When present, *S. luteus* promoted the accumulation of nutrients (e.g., Ca) in the root xylem under low external Zn concentrations (2.6–3.4 mg Zn/kg sand), while it significantly hampered their uptake under increased external Zn concentration. This result partially differs from previous results, where EMF inoculated *P. halepensis* seedlings showed increased root Ca concentration by roughly 50-fold after 1 year of high concentration of Pb-Zn-Cd exposure (Hachani et al., 2020). Such discrepancy may be due to differences in the studied plant and fungal species that have different degrees of tolerance to excess nutrients (Broadley et al., 2007; Teotia et al., 2017). By contrast, there was a significant negative relationship between Zn addition (0-1 mM) and Fe accumulation in our EMF root tissues (Fig. S3F). Similar to Zn, Fe was mostly accumulated in the fungal sheath compared to Hartig net hyphae and xylem, and Fe accumulation in the fungal sheath was also negatively affected by external Zn concentration. This indicates that an antagonistic effect between Zn concentration and Fe uptake may occur in the fungal sheath, restricting Fe translocation into root tissues and subsequently reducing Fe accumulation in the root xylem, consistent with previous studies that excess Zn decreased Fe accumulation in arbuscular mycorrhizal roots (Ibiang et al., 2017; Xie et al., 2019). However, higher Fe accumulation was observed in fungal and root tissues than Zn accumulation in the low external Zn concentration (e.g., 2.6 and 2.68 mg Zn/kg sand). The intimate association between EMF and pine roots provided the most efficient Fe solubilization and uptake, likely due to the capacity of EMF to produce siderophores that chelate and transport Fe into plant roots by their hyphae (Cress et al., 1986; Xie et al., 2019). Notably, the reference *S. luteus* genome annotation includes several putative genes associated with fungal siderophores, such as SID1 [JGI protein ID 84291; *Suillus luteus* UH-Slu-Lm8-n1], which is a putative siderophore synthetase (Kohler et al., 2015). In addition, mannoproteins, one of the dominant cell wall proteins in the EMF symbiotic interaction, can promote the retention of siderophore-Fe chelates in the cell wall, which increases Fe uptake by fungi (Martin et al., 1999; Protchenko et al., 2001). These, ultimately, may enable fungi (e.g., EMF) to absorb and transport Fe into root tissues efficiently. However, increased Zn concentration may enable Zn to outcompete Fe for chelation of limited amounts of siderophores or the ligand-binding sites in transporter proteins (Abdallah Hussein and Joo, 2019; Schalk et al., 2011; Suzuki et al., 2008), as siderophores and other transporter proteins (e.g., IRT1, ZIF1, and ZIP) may also contribute to Zn distribution and transportation (Colangelo and Guerinot, 2006; Dubeaux et al., 2018; Haydon et al., 2012; Vert et al., 2002). Yet, the main molecular mechanisms regarding the role of EMF in the regulation of Fe and Zn uptake are still elusive. The ways EMF regulate the expression of these transporter genes in the fungal sheath in response to the elevating Zn/Fe concentration should be investigated more thoroughly in future studies.

5. Conclusion

Overall, our study provides empirical evidence on how EMF regulate plant host acquisition and translocation of nutrients within root tissues in response to environmental Zn concentrations. Our results demonstrated that *S. luteus* has a promoting effect on plant nutrient acquisition (e.g., Zn, Ca, and Cu) under low external Zn concentrations, whereas it controls the uptake and transportation of these nutrients under high external Zn concentrations. The threshold of external Zn concentration to shift these dual effects of *S. luteus* on the nutrient uptake and transportation is variable for the specific nutrient. By contrast, *S. luteus* preferentially absorbed and transported Fe under low environmental Zn

concentrations, likely resulting either from the higher binding affinity of fungal siderophores for Fe or binding site out-competition by Fe in transporter proteins in low Zn conditions. Our study also provides evidence that fungal sheath serves as a barrier to regulate the transportation of Zn into the fungal Hartig net.

Although *S. luteus* in this study has the ability to protect the pine host from Zn toxicity, the magnitude of its protecting ability is still unclear, as pine seedlings all died in both EMF and non-EMF treatments under 10 mM Zn addition. Besides, as Zn is an essential element for optimal innate immune function, plants may accumulate Zn around roots to defense against certain pathogens (Djoko et al., 2015). However, how different environmental Zn concentrations affect plant immune systems is largely unknown. These knowledge gaps will be filled in our future work.

CRediT authorship contribution statement

Kaile Zhang: Software, Validation, Investigation, Resources, Formal analysis, Data curation, Writing – original draft, Funding acquisition. **Ryan Tappero:** Conceptualization, Methodology, Software, Validation, Investigation, Resources, Funding acquisition. **Joske Ruytinx:** Conceptualization, Methodology, Writing – review & editing. **Sara Branco:** Conceptualization, Methodology, Writing – review & editing, Funding acquisition. **Hui-Ling Liao:** Conceptualization, Methodology, Investigation, Resources, Writing – review & editing, Supervision, Funding acquisition.

Declaration of competing interest

The authors declare that they have no known competing financial interests or personal relationships that could have appeared to influence the work reported in this paper.

Acknowledgements

This work was supported by the DOE-BER (DE-SC0012704), BNL/NSLS-II (502981) to Hui-Ling Liao and Ryan Tappero, IOS-PBI (2029168) to Sara Branco and Hui-Ling Liao, USDA NIFA McIntire-Stennis project (1026825) to Hui-Ling Liao, and a University of Florida Graduate School Funding Award to Kaile Zhang. We thank Chih-Ming Hsu for the support and help with bioassay setup and Jan Colpaert from Hasselt University for providing a *S. luteus* culture. Parts of this research used the SRX and XFM Beamlines of the National Synchrotron Light Source II, a U.S. DOE Office of Science User Facility operated for the DOE Office of Science by Brookhaven National Laboratory under Contract No. DE-SC0012704.

Appendix A. Supplementary data

Supplementary data to this article can be found online at https://doi.org/10.1016/j.scitotenv.2021.149481.

References

Abdallah Hussein, K., Joo, J.H., 2019. Zinc ions affect siderophore production by fungi isolated from the Panax ginseng Rhizosphere. J. Microbiol. Biotechnol. 29, 105–113.

Adriaensen, K., Vrålstad, T., Noben, J.-P., Vangronsveld, J., Colpaert, J.V., 2005. Copper-adapted Suillus luteus, a symbiotic solution for pines colonizing Cu mine spoils. Appl. Environ. Microbiol. 71, 7279–7284.

Adriaensen, K., Vangronsveld, J., Colpaert, J.V., 2006. Zinc-tolerant Suillus bovinus improves growth of Zn-exposed Pinus sylvestris seedlings. Mycorrhiza 16, 553–558.

Ahmed, E., Holmström, S.J.M., 2014. Siderophores in environmental research: roles and applications. Microb. Biotechnol. 7, 196–208.

Auld, D.S., 2001. Zinc coordination sphere in biochemical zinc sites. Biometals 14, 271–313.

Broadley, M.R., White, P.J., Hammond, J.P., Zelko, I., Lux, A., 2007. Zinc in plants. New Phytol. 173, 677–702.

Bücking, H., Heyser, W., 1994. The effect of ectomycorrhizal fungi on Zn uptake and distribution in seedlings of Pinus sylvestris L. Plant Soil 167, 203–212.

Bücking, H., Kuhn, A.J., SchroÈder, W.H., 2002. The fungal sheath of ectomycorrhizal pine roots: an apoplastic barrier for the entry of calcium, magnesium, and potassium into the root cortex? J. Exp. Bot. 53, 1659–1669.

Bui, V.C., Franken, P., 2018. Acclimatization of Rhizophagus irregularis enhances Zn tolerance of the fungus and the mycorrhizal plant partner. Front. Microbiol. 9, 3156.

Butaitė, E., Baumgartner, M., Wyder, S., Kümmerli, R., 2017. Siderophore cheating and cheating resistance shape competition for iron in soil and freshwater pseudomonas communities. Nat. Commun. 8, 414.

Cabot, C., Martos, S., Llugany, M., Gallego, B., Tolrà, R., Poschenrieder, C., 2019. A role for zinc in plant defense against pathogens and herbivores. Front. Plant Sci. 10, 1171.

Canton, G.C., Bertolazi, A.A., Cogo, A.J.D., Eutrópio, F.J., Melo, J., de Souza, S.B., Krohling, A., C. E., Campostrini, 2016. Biochemical and ecophysiological responses to manganese stress by ectomycorrhizal fungus Pisolithus tinctorius and in association with Eucalyptus grandis. Mycorrhiza 26, 475–487.

Colangelo, E.P., Guerinot, M.L., 2006. Put the metal to the petal: metal uptake and transport throughout plants. Curr. Opin. Plant Biol. 9, 322–330.

Colpaert, J.V., Muller, L.A.H., Lambaerts, M., Adriaensen, K., Vangronsveld, J., 2004. Evolutionary adaptation to Zn toxicity in populations of Suilloid fungi. New Phytol. 162, 549–559.

Coninx, L., Thoonen, A., Slenders, E., Morin, E., Arnauts, N., Op De Beeck, M., Kohler, A., Ruytinx, J., Colpaert, J.V., 2017. The SlZRT1 gene encodes a plasma membrane-located ZIP (Zrt-, Irt-like protein) transporter in the ectomycorrhizal fungus Suillus luteus. Front. Microbiol. 8, 2320.

Cress, W.A., Johnson, G.V., Barton, L.L., 1986. The role of endomycorrhizal fungi in iron uptake by Hilaria jamesii. J. Plant Nutr. 9, 547–556.

Denny, H.J., Wilkins, D.A., 1987. Zinc tolerance in Betula spp. Iv. The mechanism of ectomycorrhizal amelioration of zinc toxicity. New Phytol. 106, 545–553.

Djoko, K.Y., Ong, C.-L.Y., Walker, M.J., McEwan, A.G., 2015. The role of copper and zinc toxicity in innate immune defense against bacterial pathogens. J. Biol. Chem. 290, 18954–18961.

Dubeaux, G., Neveu, J., Zelazny, E., Vert, G., 2018. Metal sensing by the IRT1 transporter-receptor orchestrates its own degradation and plant metal nutrition. Mol. Cell 69, 953–964.e5.

Gupta, N., Ram, H., Kumar, B., 2016. Mechanism of zinc absorption in plants: uptake, transport, translocation and accumulation. Rev. Environ. Sci. Technol. 15, 89–109.

Hachani, C., Lamhamedi, M.S., Cameselle, C., Gouveia, S., Zine El Abidine, A., Khasa, D.P., Béjaoui, Z., 2020. Effects of ectomycorrhizal fungi and heavy metals (Pb, Zn, and Cd) on growth and mineral nutrition of Pinus halepensis seedlings in North Africa. Microorganisms 8.

Hart, J.J., Norvell, W.A., Wel, Sullivan, L.A. L.V., Kochian, 1998. Characterization of zinc uptake, binding, and translocation in intact seedlings of bread and durum wheat cultivars. Plant Physiol. 118, 219–226.

Haydon, M.J., Kawachi, M., Wirtz, M., Hillmer, S., Hell, R., Krämer, U., 2012. Vacuolar nicotianamine has critical and distinct roles under iron deficiency and for zinc sequestration in arabidopsis. Plant Cell 24, 724–737.

Ibiang, Y.B., Mitsumoto, H., Sakamoto, K., 2017. Bradyrhizobia and arbuscular mycorrhizal fungi modulate manganese, iron, phosphorus, and polyphenols in soybean (Glycine max (L.) Merr.) under excess zinc. Environ. Exp. Bot. 137, 1–13.

Jentschke, G., Godbold, D.L., 2000. Metal toxicity and ectomycorrhizas. Physiol. Plant. 109, 107–116.

Jourand, P., Ducousso, M., Reid, R., Majorel, C., Richert, C., Riss, J., Lebrun, M., 2010. Nickel-tolerant ectomycorrhizal pisolithus albus ultramafic ecotype isolated from nickel mines in New Caledonia strongly enhance growth of the host plant Eucalyptus globulus at toxic nickel concentrations. Tree Physiol. 30, 1311–1319.

Kohler, A., Consortium, Mycorrhizal Genomics Initiative, Kuo, A., Nagy, L.G., Morin, E., Barry, K.W., Buscot, F., Canbäck, B., Choi, C., Cichocki, N., Clum, A., Colpaert, J., Copeland, A., Costa, M.D., Doré, J., Floudas, D., Gay, G., Girlanda, M., Henrissat, B., Herrmann, S., Hess, J., Högberg, N., Johansson, T., Khouja, H.-R., LaButti, K., Lahrmann, U., Levasseur, A., Lindquist, E.A., Lipzen, A., Marmeisse, R., Martino, E., Murat, C., Ngan, C.Y., Nehls, U., Plett, J.M., Pringle, A., Ohm, R.A., Perotto, S., Peter, M., Riley, R., Rineau, F., Ruytinx, J., Salamov, A., Shah, F., Sun, H., Tarkka, M., Tritt, A., Veneault-Fourrey, C., Zuccaro, A., Tunlid, A., Grigoriev, I.V., Hibbett, D.S., Martin, F., 2015. Convergent losses of decay mechanisms and rapid turnover of symbiosis genes in mycorrhizal mutualists. Nat. Genet. 47, 410–415.

Krznaric, E., Verbruggen, N., Wevers, J.H.L., Carleer, R., Vangronsveld, J., Colpaert, J.V., 2009. Cd-tolerant Suillus luteus: a fungal insurance for pines exposed to Cd. Environ. Pollut. 157, 1581–1588.

Leventhal, G.E., Ackermann, M., Schiessl, K.T., 2019. Why microbes secrete molecules to modify their environment: the case of iron-chelating siderophores. J. R. Soc. Interface 16, 20180674.

Li, L., Yan, H., Xu, W., Yu, D., Heroux, A., Lee, W.-K., Campbell, S.I., Chu, Y.S., 2017. PyXRF: Python-based X-ray fluorescence analysis package. X-Ray Nanoimaging: Instruments and Methods III. International Society for Optics and Photonics.

Liao, H.-L., Chen, Y., Vilgalys, R., 2016. Metatranscriptomic study of common and host-specific patterns of gene expression between pines and their symbiotic ectomycorrhizal fungi in the genus Suillus. PLoS Genet. 12, e1006348.

Lin, Y.-F., Aarts, M.G.M., 2012. The molecular mechanism of zinc and cadmium stress response in plants. Cell. Mol. Life Sci. 69, 3187–3206.

Maret, W., 2005. Zinc coordination environments in proteins determine zinc functions. J. Trace Elem. Med. Biol. 19, 7–12.

Martin, F., Laurent, P., de Carvalho, D., Voiblet, C., Balestrini, R., Bonfante, P., Tagu, D., 1999. Cell wall proteins of the ectomycorrhizal basidiomycete pisolithus tinctorius: identification, function, and expression in symbiosis. Fungal Genet. Biol. 27, 161–174.

Marx, D.H., 1970. The influence of ectotrophic mycorrhizal fungi on the resistance of pine roots to pathogenic infections. V. Resistance of mycorrhizae to infection by vegetative mycelium of *Phytophthora cinnamomi*. Phytopathology 60, 1472–1473.

Muller, L.A.H., Craciun, A.R., Ruytinx, J., Lambaerts, M., Verbruggen, N., Vangronsveld, J., Colpaert, J.V., 2007. Gene expression profiling of a Zn-tolerant and a Zn-sensitive Suillus luteus isolate exposed to increased external zinc concentrations. Mycorrhiza 17, 571–580.

Muller, L.A.H., Lambaerts, M., Vangronsveld, J., Colpaert, J.V., 2004. AFLP-based assessment of the effects of environmental heavy metal pollution on the genetic structure of pioneer populations of *Suillus luteus*. New Phytol. 297–303.

Mumtaz, M.Z., Ahmad, M., Jamil, M., Hussain, T., 2017. Zinc solubilizing Bacillus spp. potential candidates for biofortification in maize. Microbiol. Res. 202, 51–60.

Op De Beeck, M., Lievens, B., Busschaert, P., Rineau, F., Smits, M., Vangronsveld, J., Colpaert, J.V., 2015. Impact of metal pollution on fungal diversity and community structures. Environ. Microbiol. 17, 2035–2047.

Palmer, C.M., Guerinot, M.L., 2009. Facing the challenges of Cu, Fe and Zn homeostasis in plants. Nat. Chem. Biol. 5, 333–340.

Pella, P.A., Newbury, D.E., Steel, E.B., Blackburn, D.H., 1986. Development of National Bureau of Standards thin glass films for X-ray fluorescence spectrometry. Anal. Chem. 58, 1133–1137.

Protchenko, O., Ferea, T., Rashford, J., Tiedeman, J., Brown, P.O., Botstein, D., Philpott, C.C., 2001. Three cell wall mannoproteins facilitate the uptake of iron in Saccharomyces cerevisiae. J. Biol. Chem. 276, 49244–49250.

Read, D.J., Perez-Moreno, J., 2003. Mycorrhizas and nutrient cycling in ecosystems–a journey towards relevance? New Phytol. 157, 475–492.

Ruytinx, J., Coninx, L., Nguyen, H., Smisdom, N., Morin, E., Kohler, A., Cuypers, A., Colpaert, J.V., 2017. Identification, evolution and functional characterization of two Zn CDF-family transporters of the ectomycorrhizal fungus Suillus luteus. Environ. Microbiol. Rep. 9, 419–427.

Schalk, I.J., Hannauer, M., Braud, A., 2011. New roles for bacterial siderophores in metal transport and tolerance. Environ. Microbiol. 13, 2844–2854.

Schutzendubel, A., Polle, A., 2002. Plant responses to abiotic stresses: heavy metal-induced oxidative stress and protection by mycorrhization. J. Exp. Bot. 53, 1351–1365.

Smith, S.E., Read, D.J., 2010. Mycorrhizal Symbiosis. Academic Press.

Suzuki, M., Tsukamoto, T., Inoue, H., Watanabe, S., Matsuhashi, S., Takahashi, M., Nakanishi, H., Mori, S., Nishizawa, N.K., 2008. Deoxymugineic acid increases Zn translocation in Zn-deficient rice plants. Plant Mol. Biol. 66, 609–617.

Takeda, T.-A., Miyazaki, S., Kobayashi, M., Nishino, K., Goto, T., Matsunaga, M., Ooi, M., Shirakawa, H., Tani, F., Kawamura, T., Komai, M., Kambe, T., 2018. Zinc deficiency causes delayed ATP clearance and adenosine generation in rats and cell culture models. Commun. Biol. 1, 113.

Talbot, J.M., Bruns, T.D., Taylor, J.W., Smith, D.P., Branco, S., Glassman, S.I., Erlandson, S., Vilgalys, R., Liao, H.-L., Smith, M.E., Peay, K.G., 2014. Endemism and functional convergence across the north american soil mycobiome. Proc. Natl. Acad. Sci. U. S. A. 111, 6341–6346.

Teotia, P., Kumar, M., Prasad, R., Kumar, V., Tuteja, N., Varma, A., 2017. Mobilization of micronutrients by mycorrhizal fungi. In: Varma, A., Prasad, R., Tuteja, N. (Eds.), Mycorrhiza - Function, Diversity, State of the Art. Springer International Publishing, Cham, pp. 9–26.

Vert, G., Grotz, N., Dédaldéchamp, F., Gaymard, F., Guerinot, M.L., Briat, J.-F., Curie, C., 2002. IRT1, an Arabidopsis transporter essential for iron uptake from the soil and for plant growth. Plant Cell 14, 1223–1233.

Vinichuk, M.M., 2013. Copper, zinc, and cadmium in various fractions of soil and fungi in a Swedish forest. J. Environ. Sci. Health A Tox. Hazard. Subst. Environ. Eng. 48, 980–987.

Webb, E.C., 1992. Enzyme nomenclature 1992. Recommendations of the Nomenclature Committee of the International Union of Biochemistry and Molecular Biology on the the Nomenclature and Classification of Enzymes. Academic Press.

Xie, X., Hu, W., Fan, X., Chen, H., Tang, M., 2019. Interactions between phosphorus, zinc, and iron homeostasis in nonmycorrhizal and mycorrhizal plants. Front. Plant Sci. 10, 1172.